

From density functional theory to the functional renormalization group: superconductivity in the iron pnictide LiFeAs

Christian Platt¹, Ronny Thomale², and Werner Hanke¹

¹*Theoretical Physics, University of Würzburg, D-97074 Würzburg and*

²*Department of Physics, Princeton University, Princeton, NJ 08544*

(Dated: January 14, 2013)

A combined density functional theory and functional renormalization group method is introduced which takes into account orbital-dependent interaction parameters to derive the effective low-energy theory of weakly to intermediately correlated Fermi systems. As an application, the competing fluctuations in LiFeAs are investigated, which is the main representative of the 111 class of iron pnictides displaying no magnetic order, but superconductivity, for the parent compound. The superconducting order parameter is found to be of s_{\pm} type driven by collinear antiferromagnetic fluctuations. They eventually exceed the ferromagnetic fluctuations stemming from the small hole pocket at the Γ point, as the system flows to low energies.

PACS numbers: 74.20.Mn, 74.20.Rp, 74.25.Jb, 74.72.Jb

In recent years the renormalization group (RG) has become a much-used general concept to derive effective theories, e.g. at long length scales or for a low-energy window of a given many-particle system. For weakly to intermediately coupled fermion systems, one is mainly interested in the effective interactions near the Fermi surface (E_F), as they contain the relevant information about possibly symmetry-broken (magnetic, superconducting, etc.) or non-Fermi-liquid ground states: By systematically integrating out "high-energy" degrees of freedom one can, thus, access competing orders at low-energy or temperature in the phase diagram. The RG approaches to interacting fermions are less biased than diagrammatic summations in a particular channel (such as e.g. the RPA), as competing channels are treated on equal footing. To compute the effective interactions near E_F , many recent works use the RG flow equations for the effective action or one-particle irreducible vertex functions [1, 2] that avoid some complications of other straightforward adaptations of "Wilsonian RG" for interacting fermions [3]. These RG schemes are commonly named functional RG (FRG), as they aim at keeping as much as possible of the wave vector and frequency dependence of the vertex function, i.e. describe a flow of a coupling function rather than a flow of a finite number of coupling constants. Due to their original motivation stemming from quantum-field theory and statistical mechanics, the FRG approaches have so far been model oriented: in the high- T_c superconducting (SC) cuprates and pnictides, for example, a variety of versions of effective Hubbard-type models have been employed. They are usually confined to a reduced Hilbert space as compared to the physical system and retain only the short-range interactions as parameters.

In this work, we point out that the FRG, as a powerful scheme to resolve competing orders, can be combined with "a priori" schemes such as the density functional

theory (DFT). This new feature allows us to introduce an unbiased connection between electronic structure determinations and the competing ordering tendencies in the phase diagram. We start at "high-energy" from a local density (LDA)-type calculation. Through an evaluation of the Kohn-Sham Hamiltonian [4] between maximally-localized Wannier functions (MLWF) [5], LDA determines the bare hopping parameters of the model. Simultaneously, via a constrained screening of the direct and exchange Coulomb interactions and calculation of the corresponding MLWF matrix elements, it accounts for an "a priori" determination of the interactions. Our proposal of a DFT-FRG method still relies on some common approximations such as the use of frequency-independent effective interactions (only the full k -dependence along the Fermi surface is retained) and the neglect of the flow in the self energy, constraining its applicability to electron systems in the weak to intermediate coupling regime. For this case, however, it provides a precise treatment from ab initio parameters to a low energy description.

In this Letter, we demonstrate the usefulness of the DFT-FRG formalism for the iron based SC compound LiFeAs. Soon after the synthesis of the 1111 and 122 pnictides [6], LiFeAs as a representative of the 111 family, has been detected, with a SC phase of $T_c \sim 16\text{K}$ [7, 8]. One peculiar property of the 111 family is the absence of magnetic order in the phase diagram, while an SC instability is found already for the parent compound. From the picture of itinerant magnetism, this may be explained because of reduced nesting of the hole and electron pockets in LiFeAs as opposed to the other pnictide families where magnetic order is observed. This is suggested by band structure calculations [9] as well as by ARPES measurements on LiFeAs [10]. The latter are particularly controlled due to the simple crystal structure (tetragonal P4/nmm) and the nearly complete absence of surface states for LiFeAs [11].

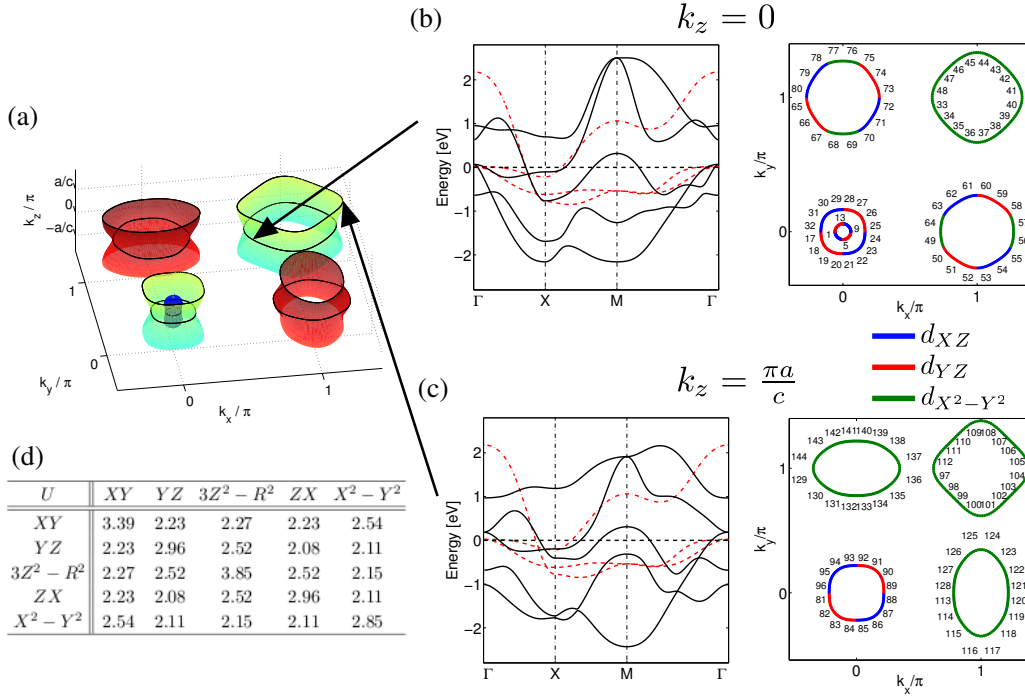


FIG. 1. (Color online). Summary of the ab-initio input on LiFeAs for the DFT-FRG. (a) 3d Fermi surface topology with visible dispersive features along z . 5-orbital band structure and Fermi surfaces for (b) $k_z = 0$ cut of the bands (Brillouin zone patches from 1 to 80) and (c) $k_z = \pi$ cut (Brillouin zone patches from 81 to 144), corresponding to the patching in the insets of Fig. 2. The red dashed lines denote the 3-band model used in [12]. Brillouin zone patches and dominant orbital weights are indicated along the Fermi surfaces. (d) Orbital dependent interaction matrix U_{ab} as obtained from cRPA calculations [13].

Despite the absence of magnetic order in LiFeAs, the role and nature of the magnetic fluctuations are still key ingredients for the SC pairing. As the material seems to reside in the intermediately coupled regime and electron-electron interactions are still important, the driving mechanism of SC is expected to originate from magnetic fluctuations [14]. Knight shift experiments, as published up to now, provide indication for strong AFM fluctuations [15]. ARPES studies, however, also point out the proximity of van Hove singularities to the Fermi level triggering ferromagnetic fluctuations [10] which is further substantiated by transport measurements [16].

A considerable body of experimental results point towards a (multi-) gap nodeless SC phase as given by NMR [17], specific heat and ARPES [18, 19] as well as microwave impedance and penetration depth measurements [20, 21]. Many aspects of the SC phase, however, in particular its order parameter symmetry, are still under current debate. While a major body of experimental evidence does not appear inconsistent with an anisotropic s_{\pm} order parameter, the fishtail effect in LiFeAs, for example, is claimed to hint p -wave SC [22]. This has also been found by an RPA mean field study of a 3-band model used to represent the LiFeAs band structure [12]. The results can be interpreted such that the small hole pocket at the Γ point, being close to a van-

Hove singularity (due to the Stoner criterion) drives the ferromagnetic fluctuations, which in turn should trigger the formation of a p -wave instability. This picture derives from the RPA and is consistent with a mean-field study where the ferromagnetic fluctuations are considered dominant. This exciting p -wave suggestion awaits still further confirmation when (beyond the RPA) competing fluctuations are taken into account and a more generic 5-orbital LiFeAs band structure as well as orbital-dependent interactions are employed. The competing magnetic fluctuations, as suggested by experimental evidence, necessitate a description which is as close to the experimental parameters as possible, taking full advantage of the high precision ab-initio electronic-structure data available. In what follows, the DFT-FRG approach takes into account the most accurate LDA data for the band structure and interactions. The FRG enables us to treat the different fluctuations of the system in an unbiased fashion (Fig. 1).

We start with the construction of an ab-initio effective Hamiltonian for our compound. As an input to our FRG calculations, we employ data from a recent work by Miyake et al., where details of the ab-initio procedure can be found [13]. The first step is a conventional band-structure calculation in the framework of LDA. From there, "target bands" are chosen around E_F , which define the band complex and the corresponding orbitals (in our

case the five d-orbitals of the Fe-3d electrons). Simultaneously, the MLWF's are extracted, which, via their matrix elements of the Kohn-Sham Hamiltonian H_{KS} , determine the transfer integrals $t_{mn}(\vec{R})$

$$t_{mn}(\vec{R}) = \langle \phi_{m\vec{0}} | H_{KS} | \phi_{n\vec{R}} \rangle. \quad (1)$$

Here $\phi_{n\vec{R}}(\vec{r})$ denotes the MLWF centered at site \vec{R} for the n -th orbital. The one-body Hamiltonian part is

$$H_0 = \sum_{i,j,\sigma} \sum_{m,n} t_{mn}(\vec{R}_i - \vec{R}_j) a_{in}^{\sigma\dagger} a_{jn}^{\sigma}, \quad (2)$$

where $a_{in}^{\sigma\dagger}$ (a_{in}^{σ}) are the creation (annihilation) operators of the MLWF with spin σ . In the second step, effective interaction parameters are extracted in terms of MLWF-matrix elements [13]. A partially screened Coulomb interaction at zero frequency $W(\vec{r}, \vec{r}'; \omega = 0)$ is calculated in the so-called cRPA, i.e. with the constraint that for the "high-energy" non-target bands RPA screening is employed [5]. Note, that the Coulomb interactions $U_{mn}(\vec{R}) = \langle \phi_{m\vec{0}} \phi_{m\vec{0}} | W | \phi_{n\vec{R}} \phi_{n\vec{R}} \rangle$ and exchange interactions $J_{mn}(\vec{R}) = \langle \phi_{m\vec{0}} \phi_{n\vec{0}} | W | \phi_{n\vec{R}} \phi_{m\vec{R}} \rangle$ are orbital dependent, comprising the interaction Hamiltonian:

$$H_I = \frac{1}{2} \sum_{\sigma\delta} \sum_{ij} \sum_{nm} \left\{ U_{mn}(\vec{R}_i - \vec{R}_j) a_{in}^{\sigma\dagger} a_{jm}^{\rho\dagger} a_{jm}^{\rho} a_{in}^{\sigma} \right. \\ \left. + J_{mn}(\vec{R}_i - \vec{R}_j) \left(a_{in}^{\sigma\dagger} a_{jm}^{\rho\dagger} a_{in}^{\rho} a_{jm}^{\sigma} + a_{in}^{\sigma\dagger} a_{in}^{\rho\dagger} a_{jm}^{\rho} a_{jm}^{\sigma} \right) \right\}. \quad (3)$$

One challenging problem of the "down-folding" is that, for entangled bands, it is not clear a priori how to "cut out" the d-subspace of the Fe-orbitals, and how to unambiguously distinguish the screening channels within the d-space from the total screening. (For a practical solution of this problem see again [5] and references therein.)

The final data of the ab-initio calculations consisting of band structure, Fermi surfaces, and bare interaction parameters are summarized in Fig. 1. The 111 compounds have a relevant dispersion orthogonal to the FeAs layers (Fig. 1a) for which we consider both the $k_z = 0$ and $k_z = \pi$ cut. The main features of the z -dispersion are the change of orbital weight along the Fermi surface as well as the absence of the small second hole pocket at Γ for $k_z = \pi$. As seen from the interaction matrix, e.g. the intra-orbital interactions (with comparably high absolute interaction scales up to 3.85 eV) differ by more than 30% between different orbitals, stressing the need to consider fully orbital-dependent parameters.

Using multi-band FRG [23–27], high-energy electronic excitations ($\varepsilon > \Lambda$) are recursively integrated out, arriving at an effective low-energy interaction or 4-point vertex function (4PF) $V(\mathbf{k}_1 n_1, \mathbf{k}_2 n_2, \mathbf{k}_3 n_3, \mathbf{k}_4 n_4)$. Here, n_1, \dots, n_4 label the different (in our case five) bands of the band complex considered and \mathbf{k}_1 to \mathbf{k}_4 the incoming and outgoing momenta. When the infrared cutoff Λ approaches the Fermi surface, a diverging renormalized

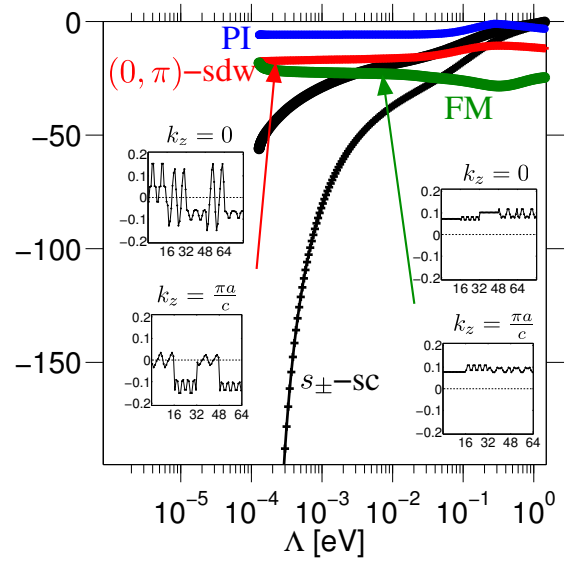


FIG. 2. (Color online). FRG temperature flow for LiFeAs. The form factors for nodal SDW and FM fluctuations are shown in the left and right inset. At cutoff scales at $\Lambda \sim 0.01$ eV the SDW becomes competitive to the previously dominant FM. The leading instability is of SC s_{\pm} type with the form factor displayed in Fig. 3.

4PF then signals a corresponding instability towards a symmetry-broken phase, with Λ_c serving as an upper bound for the transition temperature T_c . In addition, we also employ a temperature-flow FRG and compare it to the results obtained by the conventional cutoff-flow FRG [28]. At each renormalization iteration, one sums over the five one-loop diagrams [29–31], i.e. over the Cooper, spin-density wave (SDW), screening and vertex-correction channels to arrive at the renormalized vertex function. Technical details of our FRG procedure can be found elsewhere [23–25]. Due to practical limitations, approximations are made, such as the neglect of the frequency dependence of the 4-point vertex function V_{Λ} and projecting the external momenta $\mathbf{k}_1, \dots, \mathbf{k}_3$ onto the Fermi surface (with \mathbf{k}_4 being determined from momentum conservation). For a given instability characterized by some order parameter $\hat{O}_{\mathbf{k}}$ (the most important example of which is the SC instability $\hat{O}_{\mathbf{k}}^{SC} = c_{\mathbf{k}} c_{-\mathbf{k}}$ for LiFeAs), the 4PF in the particular ordering channel can be written as $\Sigma_{k,p} V_{\Lambda}(k, p) [\hat{O}_{\mathbf{k}}^{\dagger} \hat{O}_{\mathbf{p}}]$. It can be decomposed into different eigenmode contributions $V_{\Lambda}^{SC}(\mathbf{k}, -\mathbf{k}, \mathbf{p}) = \sum_i c_i^{SC}(\Lambda) f^{SC,i}(\mathbf{k}) f^{SC,i}(\mathbf{p})$ where i is an enumeration index. The leading instability of a given channel corresponds to an eigenvalue $c_1^{SC}(\Lambda)$ first diverging under the flow of Λ . $f^{SC,1}(\mathbf{k})$ is the SC form factor of the leading SC pairing mode which tells us about the pairing symmetry and, hence, gap structure. For all different ordering channels, the form factors are computed along the discretized Fermi surfaces. (Shown are the ferromagnetic (FM) and spin density wave (SDW) form factor in the

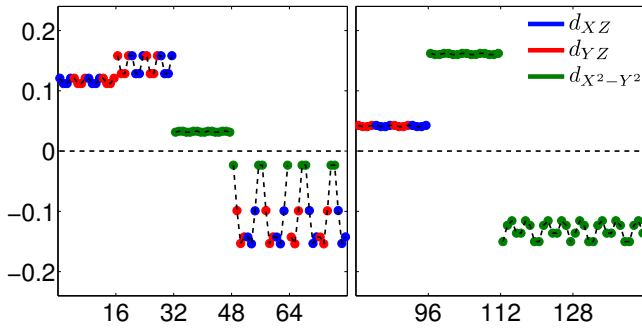


FIG. 3. (Color online). Leading SC form factor along the cuts for $k_z = 0$ and $k_z = \pi$. The dominant orbital weights for the different patches are indicated by color. The form factor shows a multi-gap nodeless anisotropic s_{\pm} order parameter.

insets of Fig. 2 as well as the SC form factor in Fig. 3.)

The flow of these leading eigenvalues of the instability channels is summarized in Fig. 2. We find that, for high cutoffs (temperatures), the FM fluctuations are dominant in correspondence to previous studies [12]. By removing the small hole pocket at Γ , we checked that it is, indeed, the main resource for FM fluctuations. At intermediate scales, however, we see in Fig. 2 that the collinear SDW fluctuations, driven by hole to electron pocket scattering along $(\pi, 0)$ and $(0, \pi)$, become competitive and finally seed an s_{\pm} instability. (This result is identically obtained both for the cutoff and the temperature flow parameter formulation. The latter is more adequate to track FM fluctuations.) From there, the vertex flow can be understood along the lines of other pnictide families [24, 25].

The form factor of the SC instability for LiFeAs is plotted in Fig. 3 along the $k_z = 0$ and $k_z = \pi$ cuts. The $k_z = 0$ cut looks typical as for other pnictide families and displays an s_{\pm} form factor changing sign between hole and electron pockets with strong anisotropy features along the electron pockets. As indicated by the dominant orbital weights along the different patches, we find from Fig. 3 that the form factor can be well understood in a scenario where the SC form factor seeks to minimize intra-orbital repulsion which is the most relevant interaction scale [32]. For $k_z = \pi$, the largest hole-pocket gap is given by the M pocket as it can scatter to the electron pockets at X through intra-orbital interactions. Since the orbital weight for these pockets is uniformly of $d_{X^2-Y^2}$ -type, the form factor anisotropies on the electron pockets are rather small.

In summary, we have introduced the DFT-FRG formalism to describe Fermi surface instabilities by taking into account a-priori DFT (LDA) band parameters and orbital-dependent interactions and providing a low-energy description in an unbiased fashion. We have applied the DFT-FRG to LiFeAs and find the leading SC instability to be of s_{\pm} -type. Within FRG, the FM fluctuations at "high temperatures" are overcome by SDW

fluctuations in the effective low-energy sector.

We thank A. Chubukov, S. Graser, M. Daghofer, I. Eremin, P. Hirschfeld, D. Scalapino, and J. van den Brink for discussions. The work was supported by DFG-SPP 1458/1 and by the Bavarian KONWIHR Program. RT is supported by the Humboldt Foundation.

-
- [1] C. Wetterich, Phys. Lett. B **301**, 90 (1993).
 - [2] M. Salmhofer and C. Honerkamp, Progr. Theor. Phys. **105**, 1 (2001).
 - [3] R. Shankar, Rev. Mod. Phys. **66**, 129 (1994).
 - [4] R. M. Dreizler and E. K. U. Gross, *Density functional theory* (Springer, Berlin, 1990).
 - [5] M. Imada and T. Miyake, J. Phys. Soc. Jpn. **79**, 112001 (2010).
 - [6] Y. Kamihara, T. Watanabe, M. Hirano, and H. Hosono, J. Am. Chem. Soc. **130**, 3296 (2008).
 - [7] X. C. Wang *et al.*, Solid State Comm. **148**, 538 (2008).
 - [8] J. H. Tapp *et al.*, Phys. Rev. B **78**, 060505 (2008).
 - [9] D. J. Singh, Phys. Rev. B **78**, 094511 (2008).
 - [10] S. V. Borisenko *et al.*, Phys. Rev. Lett. **105**, 067002 (2010).
 - [11] A. Lankau *et al.*, arXiv:1008.5234.
 - [12] P. M. R. Brydon, M. Daghofer, C. Timm, and J. van den Brink, arXiv:1009.3104.
 - [13] T. Miyake, K. Nakamura, R. Arita, and M. Imada, J. Phys. Soc. Jpn. **79**, 044705 (2010).
 - [14] There are also experimental findings which may be explained by phonon-mediated effects in LiFeAs [33, 34]; still, the consensus is that the electronic interaction scale is dominant.
 - [15] P. Jeglič *et al.*, Phys. Rev. B **81**, 140511 (2010).
 - [16] O. Heyer *et al.*, arXiv:1010.2876.
 - [17] D. S. Inosov *et al.*, Phys. Rev. Lett. **104**, 187001 (2010).
 - [18] K. Sasmal *et al.*, arXiv:1004.1387.
 - [19] U. Stockert *et al.*, arXiv:1011.4246.
 - [20] Y. Imai *et al.*, arXiv:1009.4628.
 - [21] Y. J. Song *et al.*, arXiv:1007.4906.
 - [22] A. K. Pramanik *et al.*, arXiv:1009.4896.
 - [23] R. Thomale *et al.*, Phys. Rev. B **80**, 180505 (2009).
 - [24] F. Wang *et al.*, Phys. Rev. Lett. **102**, 1047005 (2009).
 - [25] R. Thomale, C. Platt, W. Hanke, and B. A. Bernevig, arXiv:1002.3599, to appear in PRL.
 - [26] C. Platt, C. Honerkamp, and W. Hanke, New J. Phys. **11**, 055058 (2009).
 - [27] F. Wang, H. Zhai, and D.-H. Lee, Phys. Rev. B **81**, 184512 (2010).
 - [28] C. Honerkamp and M. Salmhofer, Phys. Rev. B **64**, 184516 (2001).
 - [29] C. Honerkamp, M. Salmhofer, N. Furukawa, and T. M. Rice, Phys. Rev. B **63**, 035109 (2001).
 - [30] C. J. Halboth and W. Metzner, Phys. Rev. B **61**, 7364 (2000).
 - [31] D. Zanchi and H. J. Schulz, Phys. Rev. B **61**, 13609 (2000).
 - [32] C. Platt, R. Thomale, and W. Hanke, arXiv:1012.1763.
 - [33] M. Gooch *et al.*, Eur. Phys. Lett. **85**, 27005 (2009).
 - [34] A. A. Kordyuk *et al.*, arXiv:1002.3149.